Radiation-damage-free quantum crystallography and enhanced x-ray imaging techniques using quantum multipath interference of thermal light

Zheng Li,[1,2,3,*] Tao Peng,[4] Nikita Medvedev,[5] Fenglin Wang,[2,3,1] Henry N. Chapman,[2,3,6] and Yanhua Shih[7,†]

[1]*SLAC National Accelerator Laboratory, Menlo Park, California 94025, USA*
[2]*Center for Free-Electron Laser Science, DESY, Notkestraße 85, D-22607 Hamburg, Germany*
[3]*Hamburg Centre for Ultrafast Imaging, Luruper Chaussee 149, D-22761 Hamburg, Germany*
[4]*Department of Physics, Texas A&M University, College Station, Texas 77840, USA*
[5]*Institute of Physics and Institute of Plasma Physics, Academy of Science of Czech Republic, Na Slovance 1999/2, 18221 Prague 8, Czech Republic*
[6]*Department of Physics, University of Hamburg, Jungiusstraße 9, D-20355 Hamburg, Germany*
[7]*Department of Physics, University of Maryland, Baltimore County, Baltimore, Maryland 21250, USA*

Using higher order coherence of thermal light sources, we can achieve enhancement of resolution of standard x-ray imaging techniques, such as x-ray diffraction and phase contrast imaging. The cost of implementing such schemes is minimal comparing to the schemes using entangled two-photon pairs. The proposed diffractive quantum crystallography using multipath interference of thermal light can be eventually free of radiation damage, because the diffraction pattern could be formed by using low energy photons of optical wavelength. Thus it is promising to apply the proposed quantum crystallography scheme to nanocrystalline or non-crystalline samples that are too difficult to be crystallized.

arXiv:1606.03517v3 [physics.optics] 26 Jul 2016

* zheng.li@cfel.de
† shih@umbc.edu

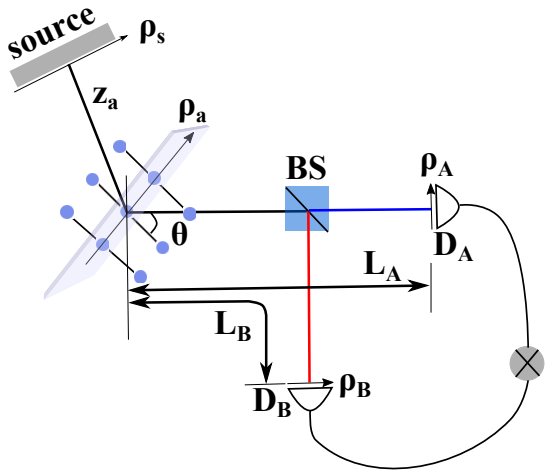

FIG. 1. Schematic description of the proposed setup for x-ray diffraction using multipath interference. photons from a thermal light source reflects from a crystal, the reflected light are divided by a beam splitter (BS) and detected jointly by two pixel detectors D_A and D_B. z_a is the distance between the source and lattice plane, θ is the reflection angle. L_A and L_B are distances from the lattice plane to the planes of pixel detectors D_A and D_B. $\vec{\rho}_s$ is a vector on the source plane, $\vec{\rho}_a$ is a vector on the lattice plane, $\vec{\rho}_A$ and $\vec{\rho}_B$ are vectors on the detector planes.

I. MOTIVATION

The Hanbury-Brown and Twiss (HBT) effect [1] was at the heart of the development of quantum optics, which fundamentally reveals the higher order coherence of a multimode thermal source. The HBT effect is a consequence of multipath interference of independent photon modes, and can be interpreted as an intrinsic quantum mechanical effect [2–7]. Here we show that using the HBT type measurements, we can enhance the resolution of conventional x-ray imaging techniques with a minimal cost. We also propose an intriguing scenario, that may could lead to crystallography using only optical photons which do not cause radiation damage to the samples. It is crucial to achieve diffractive structural determination of molecules that are too difficult to be crystallized, and can only be analyzed in the form of nanocrystal with few molecules in it or non-crystalline sample. The paper is outlined as following: we demonstrate how multipath interference can be applied to x-ray diffraction imaging and enhance the resolution in section II, and show that is could be possible to even realize diffractive crystallography with source of optical wavelength in section III. In section IV, we apply the multipath interference effect to the near-field phase contrast imaging and demonstrate the enhancement of the image contrast. And we conclude with discussion in section V.

II. ENHANCED X-RAY DIFFRACTION

According to the quantum theory of photo-detection [3, 4], an idealized pixel photodetector measures the probability of observing a photodetection event at spacetime point $(\vec{r},t)$

$$G^{(1)}(\vec{r},t) = \mathrm{tr}\left\{\hat{\rho}\hat{E}^{(-)}(\vec{r},t)\hat{E}^{(+)}(\vec{r},t)\right\}, \tag{1}$$

where $\hat{\rho}$ is the density matrix of the quantized photon field, $\hat{E}^{(-)}(\vec{r},t)$ and $\hat{E}^{(+)}(\vec{r},t)$ are the negative and positive frequency photon field operators. A joint-detection of two independent pixel photodetectors D_A and D_B measures the probability of a coincident event of two photons at spacetime points $(\vec{r}_A,t_A)$ and $(\vec{r}_B,t_B)$

$$G^{(2)}(\vec{r}_A,t_A;\vec{r}_B,t_B) = \mathrm{tr}\left\{\hat{\rho}\hat{E}^{(-)}(\vec{r}_A,t_A)\hat{E}^{(-)}(\vec{r}_B,t_B)\hat{E}^{(+)}(\vec{r}_A,t_A)\hat{E}^{(+)}(\vec{r}_B,t_B)\right\}. \tag{2}$$

A light source with spatial coherence length of l_c, which can be either a thermal light source subject to a certain propagation distance or a coherent synchrotron source can be modeled by an effective multimode photon wavefunction $|\Psi\rangle \simeq |0\rangle + \sum_{\vec{k}} f(\vec{k})\hat{a}^{\dagger}_{\vec{k}}|0\rangle$, where $f(\vec{k})$ is the probability amplitude for the radiation field to be in the single

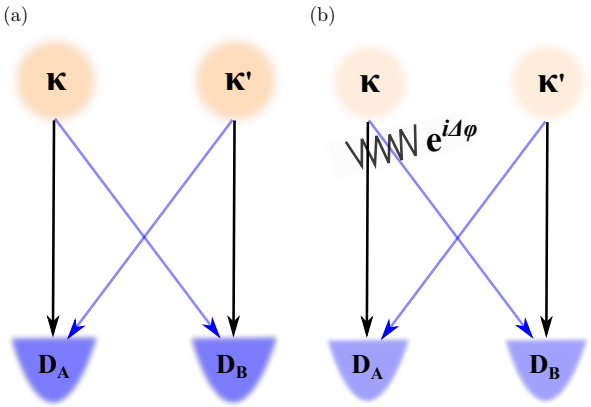

FIG. 2. (a) The two alternative yet indistinguishable paths of two single-mode photons from a thermal source, $(|1_{\vec{\kappa}}\rangle \to D_A; |1_{\vec{\kappa}'}\rangle \to D_B)$ and $(|1_{\vec{\kappa}}\rangle \to D_B; |1_{\vec{\kappa}'}\rangle \to D_A)$, the amplitudes of the two paths are added to determined the joint detection probability. (b) A phase perturbation $e^{i\Delta\varphi}$ is introduced, which models the noise in the experiment.

photon mode of wave number $\vec{k}$. Assume the transverse spatial correlation measurement is under the condition of achieving a maximal temporal coherence of $G^{(2)}(t_1 - t_2) \sim 2$, and denote $\vec{r}_j = (\vec{\rho}_j, z_j)$ and $\vec{k} = (\vec{\kappa}, \sqrt{k^2 - \kappa^2})$, the thermal light can be modeled as a mixed state with density matrix [2]

$$\hat{\rho} \simeq |0\rangle\langle 0| + \sum_{\vec{\kappa}} |f(\vec{k})|^2 |1_{\vec{\kappa}}\rangle\langle 1_{\vec{\kappa}}| + \sum_{\vec{\kappa},\vec{\kappa}'} |f(\vec{\kappa})|^2 |f(\vec{\kappa}')|^2 |1_{\vec{\kappa}} 1_{\vec{\kappa}'}\rangle\langle 1_{\vec{\kappa}} 1_{\vec{\kappa}'}|, \tag{3}$$

where we denote $|1_{\vec{\kappa}}\rangle = \hat{a}^{\dagger}_{\vec{\kappa}}|0\rangle$. The transverse part of the photon field on the two detectors D_A and D_B can be written as

$$\hat{E}^{(+)}(\vec{\rho}_j) \simeq \sum_{\vec{\kappa}} g_j(\vec{\rho}_j, z_j; \vec{\kappa}) \hat{a}_{\vec{\kappa}}, \tag{4}$$

where $g_j(\vec{\rho}_j, z_j; \vec{\kappa})$ is the Green's function for a single-mode photon. The spatial part of the second order coherence function, which is proportional to the joint photon counting rate, is thus

$$\begin{aligned} G^{(2)}(\vec{\rho}_A, z_A; \vec{\rho}_B, z_B) &= \sum_{\vec{\kappa},\vec{\kappa}'} \langle 1_{\vec{\kappa}} 1_{\vec{\kappa}'} | \hat{E}^{(-)}(\vec{\rho}_A, z_A) \hat{E}^{(-)}(\vec{\rho}_B, z_B) \hat{E}^{(+)}(\vec{\rho}_A, z_A) \hat{E}^{(+)}(\vec{\rho}_B, z_B) | 1_{\vec{\kappa}} 1_{\vec{\kappa}'} \rangle \\ &= \sum_{\vec{\kappa},\vec{\kappa}'} \left| \frac{1}{\sqrt{2}} \left[g_B(\vec{\rho}_B, z_B; \vec{\kappa}) g_A(\vec{\rho}_A, z_A; \vec{\kappa}') + g_B(\vec{\rho}_B, z_B; \vec{\kappa}') g_A(\vec{\rho}_A, z_A; \vec{\kappa}) \right] \right|^2 \\ &\equiv G^{(1)}(\vec{\rho}_A, z_A) G^{(1)}(\vec{\rho}_B, z_B) + G^{(1)*}(\vec{\rho}_A, z_A; \vec{\rho}_B, z_B; \vec{\kappa}) G^{(1)}(\vec{\rho}_A, z_A; \vec{\rho}_B, z_B; \vec{\kappa}'), \end{aligned} \tag{5}$$

where we define $G^{(1)}(\vec{\rho}_A, z_A; \vec{\rho}_B, z_B; \vec{\kappa}) = \sum_{\vec{\kappa}} g_A(\vec{\rho}_A, z_A; \vec{\kappa}) g_B^*(\vec{\rho}_B, z_B; \vec{\kappa})$. In Eq. 5, the term $G^{(1)}(\vec{\rho}_A, z_A) G^{(1)}(\vec{\rho}_B, z_B) \simeq \langle I(\vec{r}_A)\rangle \langle I(\vec{r}_B)\rangle$ gives a constant background in the joint signal intensity $\langle I(\vec{r}_A) I(\vec{r}_B)\rangle$. As shown in Fig. 2(a), the interference of pair of independent thermal photons through two alternative yet indistinguishable paths $(|1_{\vec{\kappa}}\rangle \to D_A; |1_{\vec{\kappa}'}\rangle \to D_B)$ and $(|1_{\vec{\kappa}}\rangle \to D_B; |1_{\vec{\kappa}'}\rangle \to D_A)$ is manifested as joint photon number fluctuation, through the term $G^{(1)*}(\vec{\rho}_A, z_A; \vec{\rho}_B, z_B; \vec{\kappa}) G^{(1)}(\vec{\rho}_A, z_A; \vec{\rho}_B, z_B; \vec{\kappa}') \simeq \langle \Delta I(\vec{\rho}_A) \Delta I(\vec{\rho}_B)\rangle$ in Eq. 5 [2, 5].

For the setup of x-ray diffraction shown in Fig. 1, the diffraction pattern can form in the second order measurement that is irrelevant of the spatial and temporal coherence length [8]. With these assumptions, the Green's function can be written as

$$g_j(\vec{\rho}_j, z_j; \vec{\kappa}) = \int d^2\vec{\rho}_s \int d^2\vec{\rho}_a \frac{-ik}{2\pi z_a} e^{ikz_a} e^{i\frac{k}{2z_a}|\vec{\rho}_a - \vec{\rho}_s|^2} e^{i\vec{\kappa}\cdot\vec{\rho}_s} t(\vec{\rho}_a) \frac{-ik}{2\pi L_A} e^{ikL_A} e^{i\frac{k}{2L_A}|\vec{\rho}_A - \vec{\rho}_a|^2}, \tag{6}$$

where $j = A, B$, and $t(\vec{\rho}_a) = \psi\delta(\vec{\rho}_a - \vec{r}_i)$ is the scattering amplitude of photon with the ith atom at position $\vec{r}_i$. Suppose the multipath interference imprinted in the photon number fluctuation is from scattering from atoms in two adjacent lattice plane with a distance of d and reflection angle θ, it is clear that the interference of the two indistinguishable paths can give doubled optical path difference than that from conventional Laue diffraction, which

corresponds to a resolution of $\frac{\lambda}{4}$. Denote $\delta = d\sin\theta$ and the Green's function $g_j(\vec{r}_i, \vec{\rho}_j; \vec{\kappa})$ for the propagation of a single-mode photon to detector D_j and scatters off from the atom at $\vec{r}_i$, we have

$$\begin{aligned} & G^{(1)*}(\vec{\rho}_A, z_A; \vec{\rho}_B, z_B; \vec{\kappa}) G^{(1)}(\vec{\rho}_A, z_A; \vec{\rho}_B, z_B; \vec{\kappa}') \\ = & \sum_{\vec{\kappa}} \sum_{ii'}^{\text{atoms}} g_A^*(\vec{r}_i, \vec{\rho}_A, z_A; \vec{\kappa}) g_B(\vec{r}_{i'}, \vec{\rho}_B, z_B; \vec{\kappa}) \sum_{\vec{\kappa}'} \sum_{ii'}^{\text{atoms}} g_A(\vec{r}_i, \vec{\rho}_A, z_A; \vec{\kappa}') g_B^*(\vec{r}_{i'}, \vec{\rho}_B, z_B; \vec{\kappa}') \,. \end{aligned} \tag{7}$$

Taken the summation over transverse momentum as integral, we find the following term in Eq. 7 gives the doubled optical path difference [9]

$$\begin{aligned} & \sum_{\vec{\kappa}} g_A^*(\vec{r}_2, \vec{\rho}_A, z_A; \vec{\kappa}) g_B(\vec{r}_1, \vec{\rho}_B, z_B; \vec{\kappa}) \sum_{\vec{\kappa}'} g_A(\vec{r}_1, \vec{\rho}_A, z_A; \vec{\kappa}') g_B^*(\vec{r}_2, \vec{\rho}_B, z_B; \vec{\kappa}') + \text{c.c.} \\ = & \frac{32\psi^4\pi^4}{\lambda^6 L_A^2 L_B^2 \delta^4} \cos\left[k(4\delta)\right] \,. \end{aligned} \tag{8}$$

The demonstrated scenario is consistent with that from previous study [8]. For x-ray diffraction, the doubled optical path difference in the interference kernel simply corresponds to enhanced resolution, we have the Bragg condition for the thermal light two-photon diffraction

$$4d\sin\theta = n\lambda \,, \tag{9}$$

for an integer n, which basically means that structure with period $\frac{\lambda}{4} < d < \frac{\lambda}{2}$ is able to form Bragg peaks and can thus be resolved by inverse Fourier transformation and phase retrieval techniques. Compare to the two-photon diffraction using two-photon pairs from x-ray parametric down conversion (XPDC), which has rather low photon flux, the present scheme using thermal source can be experimentally favorable. In the case of powder diffraction or femtosecond serial nanocrystallography that effectively produce a powder diffraction pattern, we can replace D_A and D_B by two pixel detectors and a sufficient large beam splitter covering the angular spread of the reflected photons, provided each pixel of the detectors are pairwise connected by a coincidence circuit, the physical scenario remains unchanged from the setup described in this section.

III. POSSIBLE ROUTE TO OPTICAL WAVELENGTH QUANTUM CRYSTALLOGRAPHY

In this section, we consider the case of two-color thermal source, with which the multipath interference effect could have the possibility to achieve crystallography with photons of only optical wavelength. Because the major obstacle of realizing diffractive structural determination of non-crystalline samples or nanocrystals, is the radiation damage of x-ray photons which ionized the sample and causing ultrafast Coulomb explosion on a sub-100 fs timescale [10]. In case we could acquire Bragg peaks from diffraction of low energy photons and atoms, we can realize the diffractive structural determination that is completely free of radiation damage. From analysis in section II, we have the complete Bragg condition for thermal light diffraction with two distinct wavelengths λ and λ'

$$2d\sin\theta(1+\frac{\lambda}{\lambda'}) + \Delta L_{AB}(1-\frac{\lambda}{\lambda'}) = n\lambda \,. \tag{10}$$

For a low energy photon with wavelength $\lambda \gg d$, Eq. 10 shows that the Bragg peaks can still be formed with an optical path compensation of ΔL_{AB}, which is a directly consequence of multipath interference and can be simply realized by fine tuning of optical arm lengths L_A and L_B. More generally, the resolution limit of quantum crystallography using thermal light is $\frac{\lambda - \Delta L_{AB}(1-\frac{\lambda}{\lambda'})}{2(1+\frac{\lambda}{\lambda'})}$.

The requirement of detector positioning with a nanometer precision could be achieved by the state-of-the-art piezoelectric actuator techniques or in a foreseeable future. For the implementation of the proposed scheme, it is crucial that the setup can be robust against the noises from all sort of sources. Because the formation of Bragg peak relies on the optical path compensation with nm precision, such that the phase shift can satisfy Eq. 10, on the other hand, the thermal instability and changes in refractive index due to air currents may introduce uncertain perturbations into the phase of the photon. However, the multipath interference can be free of these types of phase perturbation [11], which guarantees the robustness of the scheme. As shown in Fig. 2(b), the noise can be treated as an arbitrary phase to the Green's function in Eq. 5. However, the phase perturbation should have null effect to

the second order coherence function that defines the joint photodetection intensity, because [11]

$$\begin{aligned} G^{(2)}(\vec{\rho}_A,z_A;\vec{\rho}_B,z_B;\Delta\varphi) &= \sum_{\vec{\kappa},\vec{\kappa}'}\left|\frac{1}{\sqrt{2}}\left[g_B(\vec{\rho}_B,z_B;\vec{\kappa})e^{i\Delta\varphi}g_A(\vec{\rho}_A,z_A;\vec{\kappa}')+g_B(\vec{\rho}_B,z_B;\vec{\kappa}')g_A(\vec{\rho}_A,z_A;\vec{\kappa})e^{i\Delta\varphi}\right]\right|^2 \\ &= \sum_{\vec{\kappa},\vec{\kappa}'}\left|\frac{1}{\sqrt{2}}\left[g_B(\vec{\rho}_B,z_B;\vec{\kappa})g_A(\vec{\rho}_A,z_A;\vec{\kappa}')+g_B(\vec{\rho}_B,z_B;\vec{\kappa}')g_A(\vec{\rho}_A,z_A;\vec{\kappa})\right]\right|^2 \\ &\equiv G^{(2)}(\vec{\rho}_A,z_A;\vec{\rho}_B,z_B)\,, \end{aligned} \tag{11}$$

where $G^{(2)}(\vec{\rho}_A,z_A;\vec{\rho}_B,z_B)$ is invariant under phase perturbation.

It is worth to note that this effect cannot be realized by the two-photon diffraction using entangled photon pair [12], for which the optical path difference can only be 4δ. In the unfolded scheme of the entangled two-photon diffraction, the diffraction pattern is formed by the photon that scatters from the atoms finally reach the same detector and interfere with itself, this scenario does not allow optical path compensation ΔL_{AB} arises from pair of paths

$$\begin{aligned} &\left(|\vec{\kappa},\lambda\rangle \to \text{atom } 2 \to D_A; |\vec{\kappa}',\lambda'\rangle \to \text{atom } 2 \to D_B\right) \\ &\left(|\vec{\kappa},\lambda\rangle \to \text{atom } 1 \to D_B; |\vec{\kappa}',\lambda'\rangle \to \text{atom } 1 \to D_A\right)\,, \end{aligned}$$

which is the key to the diffraction pattern formation in thermal light two-photon diffraction. Although each photon does not interfere with itself in the thermal light scheme, each pair of independent photon or photon groups interferes with the pair itself [8].

As scattering with the electrons, the optical photons and the x-ray photons have very similar Thomson scattering cross sections $\frac{d\sigma(\vec{Q})}{d\Omega}=\frac{r_e^2}{2}(1+\cos^2\theta)\left|f(\vec{Q})\right|^2$, provided the optical photons are unpolarized, and r_e is the classical electron radius $r_e\simeq 2.82$ fm, Ω is the solid angle, $\vec{Q}=2\frac{\omega}{c}\sin\theta(-\cos\phi\cos\theta,-\sin\phi\cos\theta,\sin\theta)$ is the momentum transfer of the scattering, which is proportional to the photon energy ω. And $f(\vec{Q})$ is the form factor, which has a slowly varying norm dependent on photon energy. It is important to notice that the photon behaves as point particle in the elastic Thomson scattering, and its wavelength is irrelevant to the effective size of the photon, thus the optical photon does not smear out the crystal structure with period that can be much shorter than its wavelength. In fact the wavelength and the size of a quantum object reflect its wave-like and particle-like natures respectively, and should be distinguished from each other.

Because the proposed scheme can acquire Bragg peaks using low energy photons to interact with the sample, it does not introduce ionization damage to the sample, it is crucial to realize diffractive structural determination of non-crystalline samples or samples that canonly form nanocrystals with few molecules in a crystal.

IV. ENHANCED PHASE CONTRAST IMAGING

As a complementary technique to the far-field x-ray diffraction, the x-ray phase contrast imaging (PCI) is a widely applied near-field imaging technique which provide direct image of the sample [13–15]. PCI is suitable for samples that only weakly absorb photons or do not absorb photon, but only induce phase shift of the photon, the image of the sample is formed on a pixel detector with point-to-point projection. Assume the scatterer in the sample introduce a small phase shift of $\varphi\ll\pi$ to the photon (since absorption is equivalent to a phase shift of $\Delta\varphi=\pi$), the image is formed with a depth that is proportional to $\nabla^2\varphi$ [15].

PCI is in principle a near-field interference effect of the incident photon with itself that either propagates and scatters in the sample or transverses through the sample without scattering. We show here the multipath interference in the joint detector of thermal light can be applied to PCI and enhance the image depth. For the setup shown in Fig. 3, the joint intensity can be written as

$$\begin{aligned} \langle I_A(\vec{\rho}_A)I_B(\vec{\rho}_B)\rangle &= G^{(2)}(\vec{\rho}_B,\vec{\rho}_A) \\ &= G^{(1)}(\vec{\rho}_B,z_B)G^{(1)}(\vec{\rho}_A,z_A)+\left|G^{(1)}(\vec{\rho}_B,z_B,\vec{\rho}_A,z_A)\right|^2. \end{aligned} \tag{12}$$

Assume the refractive index of the sample at a point $\vec{x}$ is $n_\omega(\vec{x})=1-\delta_\omega(\vec{x})$ with $\delta_\omega(\vec{x})\ll 1$, the photon field on the detector plane at spacetime $(\vec{r}_i,t)$ can be written under Born approximation as

$$E(\vec{r}_i,\omega)=E_{\text{in}}(\vec{r}_i,\omega)-\frac{k_i^2}{2\pi}\int d^3\vec{x}'\frac{e^{ik|\vec{r}-\vec{x}'|}}{|\vec{r}-\vec{x}'|}\delta_\omega(\vec{x}')E_{\text{in}}(\vec{x}',\omega)\,, \tag{13}$$

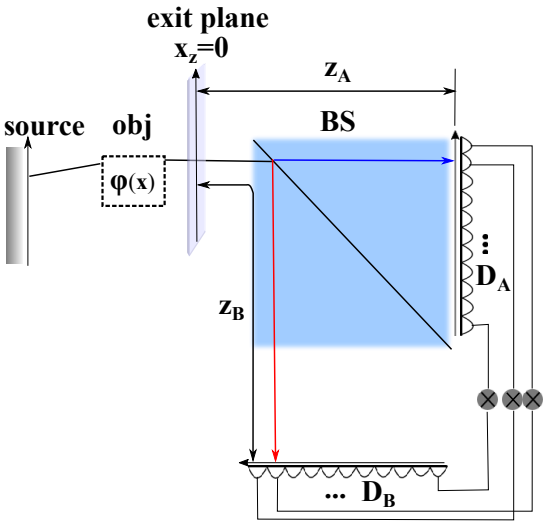

FIG. 3. The schematic configuration of phase contrast imaging using multipath interference of thermal source. The joint coincidence measurements are performed for each pair of pixels of the two detectors D_A and D_B. An artificial exit plane is assumed to be behind the sample, between which and the sample no further inhomegeneous phase shift φ that has $\nabla^2\varphi \neq 0$ will be introduced. z_i are the distances between the exit plane and pixel detectors.

where $i = A, B$. In Eq. 12, $G^{(1)}(\vec{\rho}_i, z_i; \vec{\kappa})$ is the same as conventional PCI. Define coordinates on the pixel detectors $\vec{r}_i = (\vec{\rho}_i, z_i)$, the multipath coherence function can be expressed as

$$
\begin{aligned}
& G^{(1)}(\vec{\rho}_B, z_B, \vec{\rho}_A, z_A) = \left\langle \frac{1}{2\pi}\int\int d\omega_B d\omega_A E^*(\vec{r}_B,\omega_B)E(\vec{r}_A,\omega_A)e^{-i(\omega_B-\omega_A)t} \right\rangle \\
&= \frac{1}{2\pi}\int\int d\omega_B d\omega_A \left\langle E^*_{\text{in}}(\vec{\rho}_B,\omega_B)E_{\text{in}}(\vec{\rho}_A,\omega_A)\right\rangle e^{-i(\omega_B-\omega_A)t} \\
&- \left\{ \frac{1}{2\pi}\int\int d\omega_B d\omega_A \frac{k_A^2}{2\pi}\int d^3\vec{x}' \frac{e^{ik|\vec{r}_A-\vec{x}'|}}{|\vec{r}_A-\vec{x}'|}\delta_{\omega_A}(\vec{x}')\left\langle E^*_{\text{in}}(\vec{\rho}_B,\omega_B)E_{\text{in}}(\vec{x}',\omega_A)\right\rangle e^{-i(\omega_B-\omega_A)t} \right\} \\
&- \left\{ \frac{1}{2\pi}\int\int d\omega_B d\omega_A \frac{k_B^2}{2\pi}\int d^3\vec{x}' \frac{e^{ik|\vec{r}_B-\vec{x}'|}}{|\vec{r}_B-\vec{x}'|}\delta_{\omega_B}(\vec{x}')\left\langle E^*_{\text{in}}(\vec{x},\omega_B)E_{\text{in}}(\vec{r}_A,\omega_A)\right\rangle e^{-i(\omega_B-\omega_A)t} \right\} \\
&\equiv I_{(0,0)} - I_{(0,1)} - I_{(1,0)}\,.
\end{aligned}
\tag{14}
$$

Under the condition $z_A = z_B$ and $\vec{\rho}_A = \vec{\rho}_B = \vec{\rho}$, we can straightforwardly obtain the multipath coherence function as [9]

$$
G^{(1)}(\vec{\rho}_B, z_B, \vec{\rho}_A, z_A) = I(t-\frac{z}{c})\left(1 - \frac{k}{4\pi z}\int d^2\vec{\rho}' l_c^2 e^{-\frac{k^2 l_c^2}{4z^2}|\vec{\rho}'|^2}\nabla^2\varphi(\vec{\rho}-\vec{\rho}')\right). \tag{15}
$$

The point-to-point formed image on detector plane at $\vec{\rho}$ is a convolution of the phase contrast $\nabla^2\varphi$ centered at $\vec{\rho}$ with radius $|\vec{\rho}-\vec{\rho}'|$ and a Gaussian weight. Thus the resolution of PCI is determined by requiring $e^{-\frac{k^2 l_c^2}{4z^2}p^2} \ll 1$ given $|\vec{\rho}'| = p$ as the desired resolution, i.e. the size of a single pixel. The resolution requirement leads to the condition for the coherence length

$$
\frac{z\lambda}{\pi p} \ll l_c\,, \tag{16}
$$

as well as the near-field condition $\frac{z\lambda}{p^2} \ll 1$. Provided these conditions are satisfied, we finally obtain

$$
G^{(1)}(\vec{\rho}_B, z_B, \vec{\rho}_A, z_A) = I(t-\frac{z}{c})\left(1 - \frac{z}{k}\nabla^2\varphi(\vec{\rho})\right), \tag{17}
$$

which has the same form as $G^{(1)}(\vec{\rho},z)$, and should not smear out the image contrast in the baseline signal. In the conventional PCI, the image intensity is determined by [15]

$$I(\vec{\rho},z)=G^{(1)}(\vec{\rho},z)=I\left(1-\frac{z}{k}\nabla^2\varphi(\vec{\rho})\right). \tag{18}$$

Given a coherence length l_c and incident photon wavelength, the propagation length z behind the exit plane cannot be arbitrarily extended, thus in the conventional PCI, the image depth $\frac{z}{k}\nabla^2\varphi$ cannot be simply enhanced. However, as we show in Eq. 17, the photon number fluctuation $\langle\Delta I_A(\vec{\rho})\Delta I_B(\vec{\rho})\rangle$ should not smear out the signal, instead it has the same image depth as the baseline signal $\langle I_A(\vec{\rho})\rangle\langle I_B(\vec{\rho})\rangle$, and thus we have the image intensity of joint photodetection as

$$\langle I_A(\vec{\rho})I_B(\vec{\rho})\rangle\simeq I^2\left(1-\frac{2z}{k}\nabla^2\varphi(\vec{\rho})\right), \tag{19}$$

which gives a doubled image depth. It can be expect that higher order coherence measurement of thermal light [16] can further enhance the image depth, despite of the technical difficulty of implementation.

V. DISCUSSION

In the present work, we have demonstrated that using the higher order coherence property of thermal light, we can have an easy-to-implement route to achieve enhancement of resolution for the conventional x-ray imaging techniques, both in the far- and near-field regime. We also show that the proposed multipath interference diffraction can potentially achieve radiation-damage-free crystallography or diffractive imaging of non-crystalline samples.

ACKNOWLEDGEMENTS

The authors thank Jan Malte Slowik, Xiaolei Zhu, Matthew Ware, Robert Parrish and Lida Zhang for helpful discussions. Z.L. is grateful to the Volkswagen Foundation for financial support through a Paul Ewald Fellowship.

APPENDIX A. MULTIPATH INTERFERENCE IN DIFFRACTIVE IMAGING

Here we elaborate the calculation to obtain Eq. 8. We can rewrite Eq. 8 as

$$\begin{aligned}&\sum_{\vec{\kappa}}g_A^*(\vec{r}_2,\vec{\rho}_A,z_A;\vec{\kappa})g_B(\vec{r}_1,\vec{\rho}_B,z_B;\vec{\kappa})\sum_{\vec{\kappa}'}g_A(\vec{r}_1,\vec{\rho}_A,z_A;\vec{\kappa}')g_B^*(\vec{r}_2,\vec{\rho}_B,z_B;\vec{\kappa}')\\&=G^{(1)*}(\vec{r}_2,\vec{\rho}_A.z_A;\vec{r}_1,\vec{\rho}_B,z_B;\vec{\kappa})G^{(1)}(\vec{r}_1,\vec{\rho}_A,z_A;\vec{r}_2,\vec{\rho}_B,z_B;\vec{\kappa}').\end{aligned} \tag{20}$$

Assume the photon scatters from atoms in two adjacent lattice planes of coordinates $\vec{0}$ and $\vec{d}$ and optical path lengths $z_a^{(1)}$ and $z_a^{(2)}$ from the source plane, the coherence functions can be calculated as

$$\begin{aligned}&G^{(1)*}(\vec{r}_2,\vec{\rho}_A.z_A;\vec{r}_1,\vec{\rho}_B,z_B;\vec{\kappa})\\&=\int d^2\vec{\kappa}\int d^2\vec{\rho}_a\int d^2\vec{\rho}_a'\frac{\psi^2}{\lambda^2L_AL_B}\delta(\vec{\rho}_a')\delta(\vec{\rho}_a-\vec{d})e^{-i\frac{k}{2L_A}|\vec{\rho}_A-\vec{\rho}_a|^2}e^{-i\frac{z_a^{(2)}}{2k}|\vec{\kappa}|^2}\\&\times e^{-i\vec{\kappa}\cdot\vec{\rho}_a}e^{-ik(z_a^{(2)}+L_A)}e^{i\frac{k}{2L_B}|\vec{\rho}_B-\vec{\rho}_a'|^2}e^{-i\frac{z_a^{(1)}}{2k}|\vec{\kappa}|^2}e^{i\vec{\kappa}\cdot\vec{\rho}_a'}e^{ik(z_a^{(1)}+L_B)}\\&=-i\frac{4\pi^2\psi^2}{\lambda^3L_AL_B\delta}e^{-ik(2\delta+\Delta L_{AB})}e^{-i\frac{k}{2L_A}|\vec{\rho}_A-\vec{d}|^2}e^{i\frac{k}{2L_B}|\vec{\rho}_B|^2}e^{i\frac{\delta}{2k}|\vec{d}|^2}.\end{aligned} \tag{21}$$

Similarly we can find

$$G^{(1)}(\vec{r}_1,\vec{\rho}_A.z_A;\vec{r}_2,\vec{\rho}_B,z_B;\vec{\kappa}')=i\frac{4\pi^2\psi^2}{\lambda^3L_AL_B\delta}e^{-ik(2\delta-\Delta L_{AB})}e^{i\frac{k}{2L_A}|\vec{\rho}_A-\vec{d}|^2}e^{-i\frac{k}{2L_B}|\vec{\rho}_B|^2}e^{-i\frac{\delta}{2k}|\vec{d}|^2}. \tag{22}$$

And then we arrive at Eq. 8 since

$$\begin{aligned}&G^{(1)*}(\vec{r}_2,\vec{\rho}_A.z_A;\vec{r}_1,\vec{\rho}_B,z_B;\vec{\kappa})G^{(1)}(\vec{r}_1,\vec{\rho}_A,z_A;\vec{r}_2,\vec{\rho}_B,z_B;\vec{\kappa}')\\&=\frac{16\psi^4\pi^4}{\lambda^6L_A^2L_B^2\delta^4}e^{-ik(4\delta)}.\end{aligned} \tag{23}$$

APPENDIX B. MULTIPATH INTERFERENCE IN PHASE CONTRAST IMAGING

The major task of this appendix is to elaborate the calculation to obtain Eq. 17. In Eq. 14, the coherence function describes self-interference of the incident photon that either scatters from the sample or directly transverses through the sample. Define the cross spectral density [17]

$$W(\vec{r}_1,\vec{r}_2,\omega_1,\omega_2) = \langle E^*_{\rm in}(\vec{r}_1,\omega_1)E_{\rm in}(\vec{r}_2,\omega_2)\rangle\,, \tag{24}$$

we can rewrite the $I_{(0,1)}$ term as

$$I_{(0,1)}(\vec{r}_B,\vec{r}_A) = \frac{1}{4\pi^2}\int\int \omega_B\omega_A \int d^3\vec{x}' k_A^2 \frac{e^{ik_A|\vec{r}_A-\vec{x}'|}}{|\vec{r}_A-\vec{x}'|}\delta_{\omega_A}(\vec{x}')W(\vec{r}_B,\vec{x}',\omega_B,\omega_A)e^{-i(\omega_B-\omega_A)t}\,. \tag{25}$$

Denote $\omega = \frac{\omega_A+\omega_B}{2}$, $\overline{\omega} = \omega_A - \omega_B$ and using the Huygens principle for propagating the cross spectral density from the exit plane to the detector plane [15], that

$$W(\vec{r}_B,\vec{x}',\omega,\overline{\omega}) = -\frac{1}{2\pi}\int_{x_z=0} d^2\vec{x} W(\vec{x},\vec{x}',\omega,\overline{\omega})\frac{\partial}{\partial z}\left(\frac{e^{-ik_B|\vec{r}_B-\vec{x}|}}{|\vec{r}_B-\vec{x}|}\right)\,, \tag{26}$$

where $\vec{x} = (\vec{x}_\perp, x_z = 0)$ defines the coordinate on the exit plane. The sample is assumed to be in front of the exit plane with $x_z < 0$, such that after passing the exit plane, no inhomogeneous phase shift will be introduced. Introducing the coherence length l_c of the incident photon beam, the cross spectral density $W(\vec{x},\vec{x}',\omega,\overline{\omega})$ has the form [17, 18]

$$W(\vec{x},\vec{x}',\omega,\overline{\omega}) = 2\pi\gamma(\vec{x},\vec{x}')I\delta(\overline{\omega})\delta(\omega-\omega_{\rm in})\,, \tag{27}$$

where $\gamma(\vec{x},\vec{x}') = e^{-|\vec{x}_\perp-\vec{x}'_\perp|^2/l_c^2}$ describes the transverse coherence between two points on the exit plane, a large coherence length l_c is crucial to the resolution of PCI. For thermal sources, we have $l_c = \frac{\lambda D}{a}$, where λ is the photon wavelength, D is the distance between the source and sample, and a is the source radius, it is always possible to obtain sufficient coherence length by taking a large propagation distance D. With Eqs. 26 and 27, we can further obtain

$$\begin{aligned} I_{(0,1)} = &-\frac{1}{8\pi^3}\int\int d\omega d\overline{\omega}\int d^3\vec{x}'\alpha^2(\omega+\overline{\omega}/2)^2\frac{e^{i\alpha(\omega+\overline{\omega}/2)|\vec{r}_A-\vec{x}'|}}{|\vec{r}_A-\vec{x}'|}\delta_{\omega+\overline{\omega}/2}(\vec{x}') \\ &\times\int_{x_z=0} d^2\vec{x}W(\vec{x},\vec{x}',\omega,\overline{\omega})\frac{\partial}{\partial z}\left(\frac{e^{-i\alpha(\omega-\overline{\omega}/2)|\vec{r}_B-\vec{x}|}}{|\vec{r}_B-\vec{x}|}\right)\,, \end{aligned} \tag{28}$$

where $\alpha = 1/c$ is the fine structure constant. Denote the coordinate between the exit plane and the detector as $\vec{r} = (\vec{\rho},z)$, we the relation $\frac{e^{-ik|\vec{r}-\vec{x}|}}{|\vec{r}-\vec{x}|} \simeq \frac{e^{-ik(z+|\vec{\rho}-\vec{x}_\perp|^2/2z)}}{z}$ and thus

$$\begin{aligned} I_{0,1} = &-\frac{1}{8\pi^3}\int\int d\omega d\overline{\omega}\int d^3\vec{x}'\alpha^2(\omega+\overline{\omega}/2)^2\frac{e^{i\alpha(\omega+\overline{\omega}/2)(z_A+|\vec{\rho}_A-\vec{x}'_\perp|^2/2z_A)}}{z_A}\delta_{\omega+\overline{\omega}/2}(\vec{x}') \\ &\times\int_{x_z=0} d^2\vec{x}2\pi I\gamma(\vec{x}_\perp,\vec{x}'_\perp)\delta(\omega-\omega_{\rm in})\delta(\overline{\omega})[-i\alpha(\omega-\overline{\omega}/2)]\frac{e^{-i\alpha(\omega-\overline{\omega}/2)(z_B+|\vec{\rho}_B-\vec{x}'_\perp|^2/2z_B)}}{z_B}e^{i\overline{\omega}t} \\ = &-iI\frac{k^2}{4\pi^2 z_A z_B}\int d^2\vec{x}'_\perp\int_{x_z=0} d^2\vec{x}_\perp\gamma(\vec{x}_\perp,\vec{x}'_\perp)\left\{-k\int dx'_z\delta_\omega(\vec{x}')\right\}e^{ik\left(\frac{|\vec{\rho}_A-\vec{x}'_\perp|^2}{2z_A}-\frac{|\vec{\rho}_B-\vec{x}_\perp|^2}{2z_B}\right)}e^{ik(z_A-z_B)}\,, \end{aligned} \tag{29}$$

where we denote $\omega \equiv \omega_{\rm in}$. The accumulated phase shift for a photon that travels through the sample and arrives at the exit plane is defined as

$$\varphi(\vec{x}'_\perp) = -k\int dx'_z\delta_\omega(\vec{x}')\,, \tag{30}$$

with which we write $I_{(0,1)}$ as

$$I_{(0,1)} = -iI\frac{k^2}{4\pi^2 z^2}\int d^2\vec{x}'_\perp\int d^2\vec{x}_\perp\gamma(\vec{x}_\perp,\vec{x}'_\perp)\varphi(\vec{x}'_\perp)e^{i\frac{k}{2}\left(\frac{|\vec{\rho}_A-\vec{x}'_\perp|^2}{z_A}-\frac{|\vec{\rho}_B-\vec{x}_\perp|^2}{z_B}\right)}e^{ik(z_A-z_B)}\,. \tag{31}$$

Similarly we found the term $I_{(1,0)}$ as

$$I_{(1,0)} = iI\frac{k^2}{4\pi^2 z^2}\int d^2\vec{x}'_\perp \int d^2\vec{x}_\perp \gamma(\vec{x}_\perp,\vec{x}'_\perp)\varphi(\vec{x}'_\perp)e^{i\frac{k}{2}\left(-\frac{|\vec{\rho}_B-\vec{x}'_\perp|^2}{z_B}+\frac{|\vec{\rho}_A-\vec{x}_\perp|^2}{z_A}\right)}e^{-ik(z_A-z_B)} \tag{32}$$

As shown in Fig. 3, the pixels of the two detectors are pairwise connected through coincidence circuit, we can thus assume $\vec{\rho}_A = \vec{\rho}_B \equiv \vec{\rho}$. We denote

$$\begin{aligned}\frac{z_B - z_A}{z_A z_B} &= \frac{-\eta}{z}\\ \frac{z_B + z_A}{z_A z_B} &= \frac{2\zeta}{z}\\ z_{AB} &= z_A - z_B\,,\end{aligned} \tag{33}$$

where for the case $z_A = z_B = z$, we have $\eta = 0, \zeta = 1, z_{AB} = 0$. The interference kernel of the coherence function is thus

$$\begin{aligned}I_{(0,1)} + I_{(1,0)} = -iI\frac{k^2}{4\pi^2 z^2}\int d^2\vec{a}\int d^2\vec{b}\left[e^{-\left(\frac{1}{l_c^2}+i\frac{k\eta}{8z}\right)b^2}\right]e^{-i\frac{\eta k}{4z}a^2 + i\frac{\eta k}{2z}\vec{\rho}\cdot\vec{a}}\\ \times\,\varphi(\vec{a}-\vec{b}/2)\left[e^{-i\frac{\zeta k}{z}(\vec{a}-\vec{\rho})\cdot\vec{b}}e^{-ikz_{AB}} - e^{i\frac{\zeta k}{z}(\vec{a}-\vec{\rho})\cdot\vec{b}}e^{ikz_{AB}}\right],\end{aligned} \tag{34}$$

where $\vec{a} = \frac{1}{2}(\vec{x}_\perp + \vec{x}'_\perp)$ and $\vec{b} = \vec{x}_\perp - \vec{x}'_\perp$. Further taken transformation $\vec{a} \equiv \vec{a} - \vec{b}/2$, we have

$$\begin{aligned}I_{(0,1)} + I_{(1,0)} = -iI\frac{k^2}{4\pi^2 z^2}\int d^2\vec{b}\int d^2\vec{a}e^{-i\left(\frac{1}{l_c^2}+i\frac{\eta k}{8z}\right)b^2}\varphi(\vec{a})\left\{e^{-i\frac{\eta k}{4z}[(\vec{a}+\vec{b}/2+\vec{\rho})^2-\rho^2]}e^{i\frac{\zeta k}{z}(\vec{a}\cdot\vec{b}-\vec{\rho}\cdot\vec{b})-ikz_{AB}}e^{i\frac{\zeta k}{2z}b^2}\right.\\ \left. - e^{-i\frac{\eta k}{4z}[(\vec{a}-\vec{b}/2+\vec{\rho})^2-\rho^2]}e^{i\frac{\zeta k}{z}(\vec{a}\cdot\vec{b}-\vec{\rho}\cdot\vec{b})+ikz_{AB}}e^{-i\frac{\zeta k}{2z}b^2}\right\}.\end{aligned} \tag{35}$$

Taken the simplest case $z_A = z_B$, we have

$$\begin{aligned}I_{(0,1)} + I_{(1,0)} &= I\frac{k^2}{2\pi^2 z^2}\int d^2\vec{b}\int d^2\vec{a}e^{-\frac{b^2}{l_c^2}}\varphi(\vec{a})e^{-i\frac{k}{z}\vec{\rho}\cdot\vec{b}}e^{i\frac{k}{z}\vec{b}\cdot\vec{a}}\sin\left(\frac{k}{2z}b^2\right)\\ &\simeq I\frac{k^2}{\pi z^2}\int d^2\vec{b}e^{-\frac{b^2}{l_c^2}}[\mathscr{F}\varphi](\frac{k}{z}\vec{b})\frac{k}{2z}b^2e^{-i\frac{k}{z}\vec{\rho}\cdot\vec{b}}.\end{aligned} \tag{36}$$

Define transformation $\vec{b} = \frac{k}{z}\vec{b}$,

$$\begin{aligned}I_{(0,1)} + I_{(1,0)} &= I\frac{z}{2\pi k}\int d^2\vec{b}e^{-\frac{z^2b^2}{k^2l_c^2}}[\mathscr{F}\nabla^2\varphi](\vec{b})e^{-i\vec{\rho}\cdot\vec{b}}\\ &= I\frac{z}{4\pi^2 k}\left\{\mathscr{F}^{-1}\left(e^{-\frac{z^2b^2}{k^2l_c^2}}\right)\otimes\mathscr{F}^{-1}\left[\mathscr{F}\nabla^2\varphi\right]\right\}(\vec{\rho})\\ &= I\frac{z}{2\pi k}\int d^2\vec{\rho}'\frac{k^2l_c^2}{2z^2}e^{-\frac{k^2l_c^2}{4z^2}|\vec{\rho}'|^2}\nabla^2\varphi(\vec{\rho}-\vec{\rho}')\,,\end{aligned} \tag{37}$$

define $\vec{y}' = \frac{kl_c}{2z}\vec{\rho}'$, we have

$$I_{(0,1)} + I_{(1,0)} = I\frac{z}{\pi k}\int d^2\vec{y}'e^{-y'^2}\nabla^2\varphi(\vec{\rho}-\frac{2z}{kl_c}\vec{y}') \tag{38}$$

For sufficiently large l_c, which guarantees rapid decaying of the convolution factor that satisfies $e^{-y'^2} \ll 1$ with given pixel size (resolution) $|\vec{\rho}'| = p$, Eq. 39 reduces to

$$I_{(0,1)} + I_{(1,0)} = I\frac{z}{k}\nabla^2\varphi(\vec{\rho}) \tag{39}$$

[1] R. Hanbury-Brown and R. Q. Twiss, Nature **177**, 27 (1956).
[2] Y. H. Shih, *An introduction to quantum optics* (CRC press, 2011).
[3] R. J. Glauber, Phys. Rev. **130**, 2529 (1963).
[4] R. J. Glauber, Phys. Rev. **131**, 2766 (1963).
[5] T. Jeltes, J. M. McNamara, W. Hogervorst, W. Vassen, V. Krachmalnicoff, M. Schellekens, A. Perrin, H. Chang, D. Boiron, A. Aspect, *et al.*, Nature **445**, 402 (2007).
[6] U. Fano, Am. J. Phys. **29**, 539 (1961).
[7] G. Baym, Acta Phys. Pol. B **29**, 1839 (1998).
[8] G. Scarcelli, A. Valencia, and Y. Shih, EPL (Europhysics Letters) **68**, 618 (2004).
[9] Appendix.
[10] A. Barty, C. Caleman, A. Aquila, N. Timneanu, L. Lomb, T. A. White, J. Andreasson, D. Arnlund, S. Bajt, T. R. M. Barends, M. Barthelmess, M. J. Bogan, C. Bostedt, J. D. Bozek, R. Coffee, N. Coppola, J. Davidsson, D. P. DePonte, R. B. Doak, T. Ekeberg, V. Elser, S. W. Epp, B. Erk, H. Fleckenstein, L. Foucar, P. Fromme, H. Graafsma, L. Gumprecht, J. Hajdu, C. Y. Hampton, R. Hartmann, A. Hartmann, G. Hauser, H. Hirsemann, P. Holl, M. S. Hunter, L. Johansson, S. Kassemeyer, N. Kimmel, R. A. Kirian, M. Liang, F. R. N. C. Maia, E. Malmerberg, S. Marchesini, A. V. Martin, K. Nass, R. Neutze, C. Reich, D. Rolles, B. Rudek, A. Rudenko, H. Scott, I. Schlichting, J. Schulz, M. M. Seibert, R. L. Shoeman, R. G. Sierra, H. Soltau, J. C. H. Spence, F. Stellato, S. Stern, L. Strüder, J. Ullrich, X. Wang, G. Weidenspointner, U. Weierstall, C. B. Wunderer, and H. N. Chapman, Nature Photonics **6**, 35 (2012).
[11] R. E. Meyers, K. S. Deacon, and Y. H. Shih, Appl. Phys. Lett. **98**, 111115 (2011).
[12] M. D'Angelo, M. V. Chekhova, and Y. Shih, Phys. Rev. Lett. **87**, 013602 (2001).
[13] G. Dixit, J. M. Slowik, and R. Santra, Phys. Rev. Lett. **110**, 137403 (2013).
[14] J. M. Slowik and R. Santra, J. Phys. B: Atomic, Molecular and Optical Physics **46**, 164016 (2013).
[15] D. Paganin, *Coherent X-ray optics* (Oxford University Press, 2006).
[16] S. Oppel, T. Büttner, P. Kok, and J. von Zanthier, Phys. Rev. Lett. **109**, 233603 (2012).
[17] H. Lajunen, A. T. Friberg, and P. Östlund, J. Opt. Soc. Am. A **23**, 2530 (2006).
[18] P. Pääkkönen, J. Turunen, P. Vahimaa, A. T. Friberg, and F. Wyrowski, Opt. commun. **204**, 53 (2002).